ACADEMIA ROMÂNĂ
Revue Roumaine de Chimie
http://web.icf.ro/rrch/

Rev. Roum. Chim.,
2016, *61*(8-9), 711-719

Dedicated to Professor Claude Nicolau on the occasion of his 80th anniversary

A DFT STUDY ON 2-(HYDROXY-2-BENZYLIDENE)-CYCLOHEXANONE***

Iulia PĂUŞESCU,[a] Mihai MEDELEANU[b,*] Raluca-Oana POP,[c] Zeno SIMON[a**] and Otilia COSTIŞOR[a]

[a]Institute of Chemistry Timişoara of Roumanian Academy, 24 Mihai Viteazul Bvd, 300223, Timişoara, Roumania
[b]University Politehnica Timişoara, Faculty of Industrial Chemistry and Environmental Engineering, 6 Vasile Parvan Bvd, 300223, Timişoara, Roumania
[c]University of Medicine and Pharmacy Victor Babeş Timişoara, Faculty of Pharmacy, 2 Eftimie Murgu Square, 300041, Timişoara, Roumania

Received November 12, 2015

The 2-(2-hydroxy-benzylidene)-cyclohexanone (HBC) was synthesized. Theoretical calculations of geometrical structure, vibrational wavenumbers and absorption wavelengths of HBC were carried out with the DFT method at B3LYP/6-311+G(d,p) level of theory. The optimized geometrical parameters obtained by DFT calculations are in good agreement with X-ray diffraction values for a similar structure. The theoretically computed vibrations show a good correlation with the recorded spectral data. The energy and oscillator strength calculated by time-dependent density functional theory (TD-DFT) results reveal a good correlation of the absorption bands positions with the experimental findings. The HOMO-LUMO energy gap, Mulliken polpulation on atomic charges and NBO analysis were also calculated.

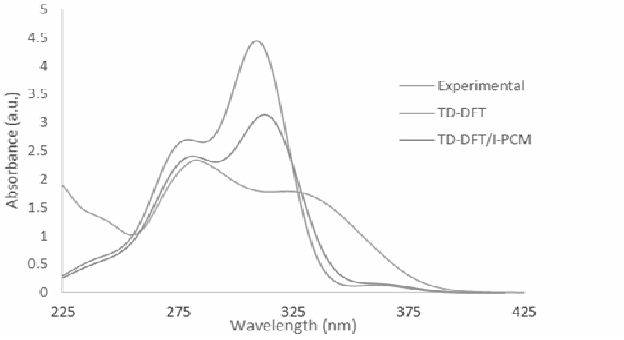

INTRODUCTION

Molecular level systems able to switch between two different states by using external stimulus are the subject of interest since they can be used for applications in optoelectronic devices, such as memories and switches.[1,2] By using a single input, a chemical compound can play between two states. When more than one input is used, the number of available states increases, leading to systems capable of performing complex functions.[3] Typical examples of such bistable systems are the so-called photochromic compounds, where the input causing the switching between the two species is the light. This external stimulus has attracted much attention since it can be localized in time and space and it can also be triggered from outside of the system.[4]

* Corresponding author: mihai.medeleanu@upt.ro
** Deceased in 2015
*** Supporting information on http: //web.icf.ro/rrch/ or http: //revroum.lew.ro

The cyclo-conjugated di-benzylideneketone families of compounds, symmetric and asymmetric, have undergone intensive research, owing to their network of chemical transformations when submitted to different stimuli, for example light and pH.[5-9] The asymmetric compounds in the presence of external stimuli undergo more intermediary states than the symmetric ones, which makes them more appealing not only for fundamental research, but also for nanoscience and nanotechnology. In order to obtain and characterize such asymmetric compounds, a key step is the synthesis of the mono-substituted benzylidene cyclohexanone derivative.

In the present study, we have synthesized and characterized an intermediate for di-benzylidene asymmetric compounds, 2-(2-hydroxy-benzylidene)-cyclohexanone (HBC), a mono-substituted benzylidene cyclohexanone derivative (which itself could exhibit photochromic behavior due to its structural features). In order to evaluate the possibility of this compound to exhibit photochromic behavior, theoretical calculations have been carried out by DFT methods at B3LYP/6-311+G(d,p) level of theory to correlate the experimental and theoretical IR and UV spectral characteristics of the studied compound. In addition, HOMO-LUMO energy gap, Mulliken population on atomic charges and NBO analysis have been used to elucidate the information on the structural and bonding features and electron delocalization within the molecule.

RESULTS AND DISCUSSION

Geometry optimization

The geometry optimization of HBC was performed at B3LYP/6-311+G(d,p) level of theory. The optimized structure is presented in Fig. 1. From frequency calculation it was proven that the structure corresponds to an energy minimum due to the fact that there are no imaginary frequencies. The calculated structural parameters, bond lengths and bond angles, along with X-ray diffraction values for a similar structure, 2-(4-dimethylamino-benzylidene)-cyclohexanone,[10] are given in Table 1. For HBC there are no available X-ray diffraction data reported in literature.

The cyclohexanone ring, depending on the substitution or lack thereof, is generally constrained to either the chair (energetically favored) or the boat conformer.[11,12] In HBC, the cyclohexanone ring has a slightly changed chair conformation with one side (C_{13}, C_{11}, C_9) a little bit flattened with a dihedral angle 20.2° and the other side (C_8, C_{10}, C_{12}) with chair conformation with a dihedral angle -61.2°. The dienone system has a higher degree of conjugation due to the electron-donating effect of the hydroxyl group, which results in the flattening at one end (C_{11}).

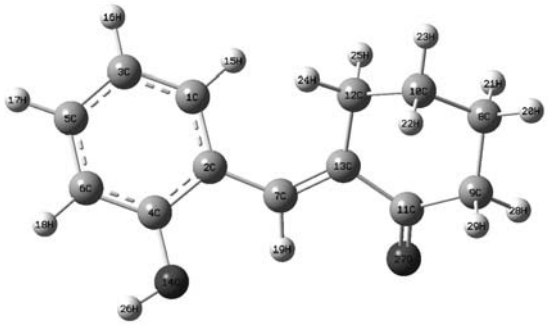

Fig. 1 – The optimized structure of HBC at B3LYP/6-311+G(d,p) level of theory.

Table 1

Comparison between optimized geometric data for HBC at B3LYP/6-311+G(d,p) level of theory and 2-(4-dimethylamino-benzylidene)-cyclohexanone[a]

Bond lengths (Å)			Bond angles (°)		
	calculated	experimental[a]		calculated	experimental[a]
$C_1 - C_2$	1.404	1.398	$C_2 - C_1 - C_3$	121.94	122.9
$C_2 - C_4$	1.412	1.401	$C_1 - C_3 - C_5$	119.60	115.8
$C_4 - C_6$	1.394	1.398	$C_3 - C_5 - C_6$	119.96	121.9
$C_5 - C_6$	1.392	1.382	$C_5 - C_6 - C_4$	120.15	121.4
$C_3 - C_5$	1.393	1.398	$C_6 - C_4 - O_{14}$	121.75	121.4
$C_1 - C_3$	1.391	1.402	$C_6 - C_4 - C_2$	121.08	117.0
$C_4 - O_{14}$	1.366	1.374	$O_{14} - C_4 - C_2$	117.16	121.5

Table 1 (continued)

$C_2 - C_7$	1.464	1.453	$C_4 - C_2 - C_1$	117.23	120.9
$C_7 - C_{13}$	1.351	1.347	$C_4 - C_2 - C_7$	118.93	115.8
$C_{12} - C_{13}$	1.516	1.504	$C_2 - C_7 - C_{13}$	129.05	131.8
$C_{10} - C_{12}$	1.535	1.523	$C_7 - C_{13} - C_{11}$	115.90	116.0
$C_8 - C_{10}$	1.528	1.508	$C_{13} - C_{11} - O_{27}$	121.92	119.2
$C_8 - C_9$	1.532	1.522	$O_{27} - C_{11} - C_9$	119.81	119.0
$C_9 - C_{11}$	1.524	1.505	$C_{11} - C_9 - C_8$	115.03	115.5
$C_{11} - O_{27}$	1.218	1.220	$C_9 - C_8 - C_{10}$	110.41	109.3
$C_{11} - C_{13}$	1.504	1.494	$C_8 - C_{10} - C_{12}$	110.81	110.0
			$C_{10} - C_{12} - C_{13}$	113.45	113.9
			$C_{12} - C_{13} - C_7$	125.36	124.9

[a] From ref.[10]

Vibrational spectral analysis

The experimental and computed FT-IR spectra of HBC are given in Fig. 2. The calculated vibrational wavenumbers and the measured infrared band positions and their assignments are given in Table 2.

Phenyl ring vibrations

The aromatic C–H stretching vibrations in benzene rings are generally observed in the region 3100–3000cm^{-1}.[13,14] In the present work the experimental FT-IR band at 2937 cm^{-1} is assigned to the aromatic C – H stretching vibration. The theoretically computed vibrations by B3LYP/6-311+G(d,p) for the C – H are predicted at 3066 cm^{-1} ($C_3 - H_{16}$, $C_5 - H_{17}$ – sym. stretch), 3028 cm^{-1} ($C_6 - H_{18}$), 3081 cm^{-1} ($C_1 - H_{15}$, $C_3 - H_{16}$) and 3053 cm^{-1} ($C_3 - H_{15}$, $C_5 - H_{17}$ – asym stretch) and are in good agreement with the recorded spectral data.

The C – H in-plane bending vibrations appear in the region 1300 – 1000 cm^{-1}.[13,14] The C – H in-plane bending vibration computed at 1276, 1228, 1178, 1147, 1137 cm^{-1} show a good correlation with the experimental FT-IR band at 1249 cm^{-1}.

The absorption bands from the C – H out-of-plane bending vibrations are observed in the region 1000 – 675 cm^{-1}.[13,14] The FT-IR band at 750 cm^{-1} is assigned to the C – H out-of-plane bending vibration, while the theoretically computed values for this vibration are at 926, 821 and 731 cm^{-1}.

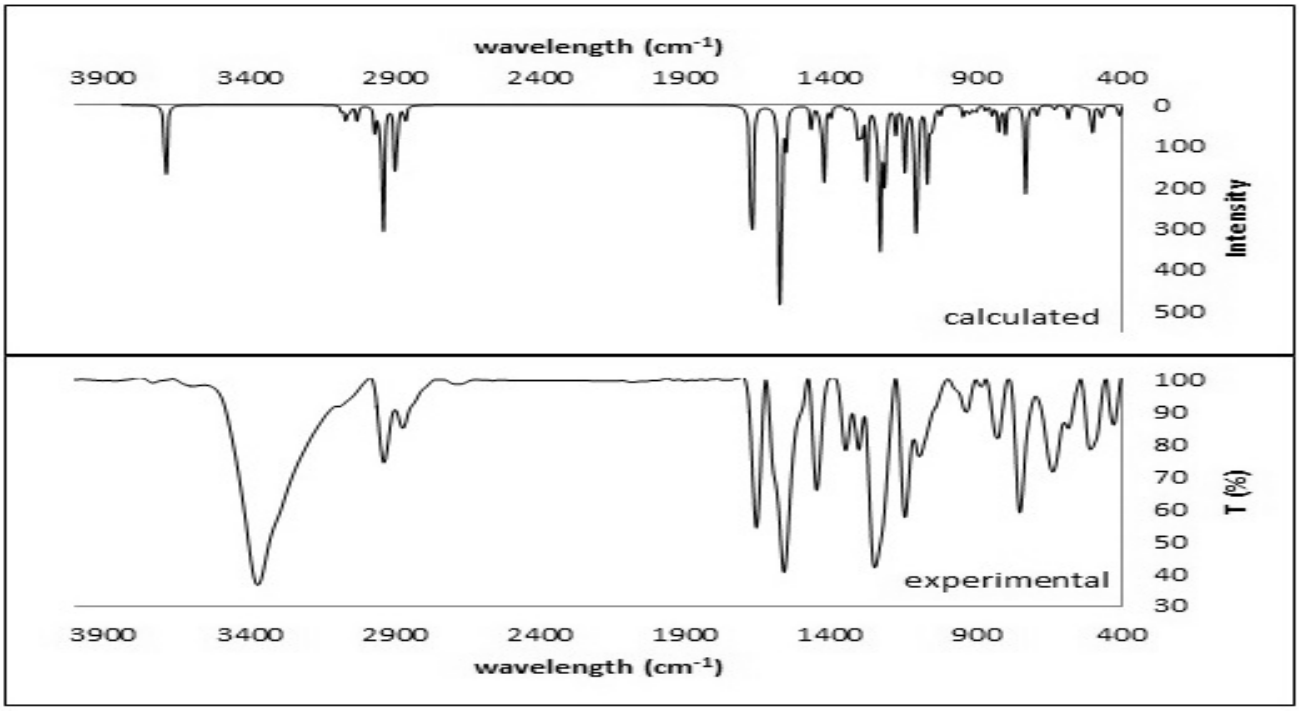

Fig. 2 – The calculated and the experimental IR spectra of HBC.

Table 2

Measured FT-IR and computed vibrational bands for HBC and their assignments

$\nu_{IR}(cm^{-1})$	$\nu_{cal}(cm^{-1})$	IR intensity	Assignment
3370	3687	79.8	$O_{14} – H_{26}$ stretch
2937	3066	15.8	$C_3 – H_{16}$ and $C_5 – H_{17}$ symmetric stretch
	3028	14.3	$C_6 – H_{18}$ stretch
2871	2941	46.2	$H_{22} – C_{10} – H_{23}$ asymmetric stretch
	2938	61	$H_{20} – C_8 – H_{21}$ asymmetric stretch
	2899	41.1	$H_{22} – C_{10} – H_{23}$ and $H_{20} – C_8 – H_{21}$ symmetric stretch
1655	1672	166.3	$C_{11} – O_{27}$ stretch
1561	1573	205.9	$C_7 – C_{13}$ stretch
1449	1424	61.1	$C_{ar} – H$ stretch
1348	1309	23.4	CH_2 wagging
1303	1300	15.7	CH_2 wagging
	1292	16.7	CH_2 wagging
1249	1276	53.9	C – H ipb in the phenyl ring
	1233	56.2	CH_2 twisting (C_9)
	1228	83.5	C – O ipb in phenyl ring
1145	1213	61.6	CH_2 twisting (C_{12}, C_{10}, C_8, C_9)
	1147	48.7	C – H ipb in the phenyl ring
1095	1109	106.9	CH_2 twisting (C_{12}, C_{10}, C_8, C_9)
	1100	34.1	CH_2 twisting (C_{12}, C_{10}, C_8, C_9)
934	1069	54.3	C – H ipb in the phenyl ring
826	800	20.9	CH_2 rocking (C_{12}, C_{10}, C_8, C_9)
750	731	67.3	C – H opb in the phenyl ring
582	583	11.1	CH_2 rocking (C_{12}, C_{10}, C_8, C_9)
508	542	28.9	C – H ipb in the phenyl ring and CH_2 rocking
428	393	93.6	$O_{14} – H_{26}$ opb

Vibrations of cyclohexanone

The vibrational spectrum of liquid cyclohexanone was thoroughly investigated along with a normal coordinate analysis.[15] The asymmetric and symmetric stretching corresponding to CH_2 is observed in the FT-IR spectrum at 2871 cm^{-1}. The vibrations for the asymmetric stretching were computed at 2941 cm^{-1} (C_{10}), 2938 cm^{-1} (C_8) and for the symmetric stretching at 2899 cm^{-1}. The wagging vibrations in the experimental spectrum can be observed at 1348 and 1303 cm^{-1}, while the theoretically values are at 1309, 1300 and 1292 cm^{-1}. The CH_2 twisting mode are found in the recorded spectrum at 1145 and 1095 cm^{-1}, while the predicted values for these vibration are at 1213, 1147, 1109 and 1100 cm^{-1}, showing a good correlation with the experimental data. The CH_2 rocking vibration in the FT-IR spectrum is at 826 cm^{-1} and the computed one at 800 cm^{-1}.

The carbonyl stretching vibrations in ketones are usually expected in the region 1715 – 1680 cm^{-1}.[14] In HBC the carbonyl stretching vibration is observed at 1655 cm^{-1} and calculated at 1672 cm^{-1}. The higher degree of conjugation in HBC causes an increased single bond character of the carbonyl bond,[16] and consequently lowers the wavenumber of the group.[14]

O – H vibrations

The hydroxyl group has three types of vibrations: stretching, in plane and out of plane bending vibrations. The free O – H stretching vibrations are generally observed around 3500 cm^{-1},[17] while the associated group absorbs in the range 3200 – 3250 cm^{-1}, due to intermolecular hydrogen bonding.[18] In our case the strong band in the FT-IR spectrum at 3370 cm^{-1} is assigned to the O – H stretching, lowered due to strong intermolecular hydrogen bonding. The theoretically computed value at B3LYP/6-311+G(d,p) level for the O – H stretching vibration is at 3687 cm^{-1}. Because the predicted vibrational spectrum was computed in the gas phase, this band corresponds to the free O – H vibration. The hydroxyl in-plane bending vibration in phenols are found in the region 1150 – 1250 cm^{-1}.[17] HBC FT-IR spectrum presents a strong band at 1249 cm^{-1} which was assigned to the O – H in-plane bending. The computed value of this vibration is at 1228 cm^{-1}, in good agreement to the experimental value.

Electronic spectra analysis

The UV-Vis absorption spectrum was measured on a $2 \cdot 10^{-4}$M solution of 2-(2-hydroxy-benzylidene)-

cyclohexanone in methanol. Time-dependent DFT (TD-DFT) calculations were performed on the optimized structure of HBC. The lowest six, eight, ten and twenty singlet→singlet spin allowed excited states were taken into account. The electronic absorption spectra were computed in vacuum and in methanol with the PCM model which takes into account the solvent effects that modify the UV spectra. The results showed very small differences, so only the six singlet→singlet spin allowed excited states calculations are presented. The experimental and the simulated UV-Vis spectra of HBC are given in Fig. 3. For all calculations the 6-311+G(d,p) basis set was used.

The experimental peaks, the calculated excitation energies, E(eV), the oscillator strength, f, and the absorption wavelength for the lowest six singlet→singlet spin allowed excited states are given in Table 3.

The calculated excitation energies, E(eV), the oscillator strength, f, and the absorption wavelength for the lowest eight, ten and twenty singlet→singlet spin allowed excited states are given in Supporting information.

The experimental UV-Vis spectrum shows two absorption bands at 284 nm and 330 nm. Both types of theoretical calculations show two moderately intense bands around the values obtained from experimental measurements. For the predictions in vacuum, the bands are at 314 nm with an oscillator strength of 0.30334 corresponding to the HOMO to LUMO transition, and one at 278 nm with an oscillator strength of 0.2224 corresponding to the HOMO-2 to LUMO transition. With the PCM method the absorption bands were computed at 309 nm with an oscillator strength of 0.3454, corresponding to the HOMO to LUMO transition, and at 275 nm with an oscillator strength of 0.1855, corresponding to the HOMO-2 to LUMO transition. The results of both theoretical calculations reveal a good correlation of the absorption bands positions with the experimental data.

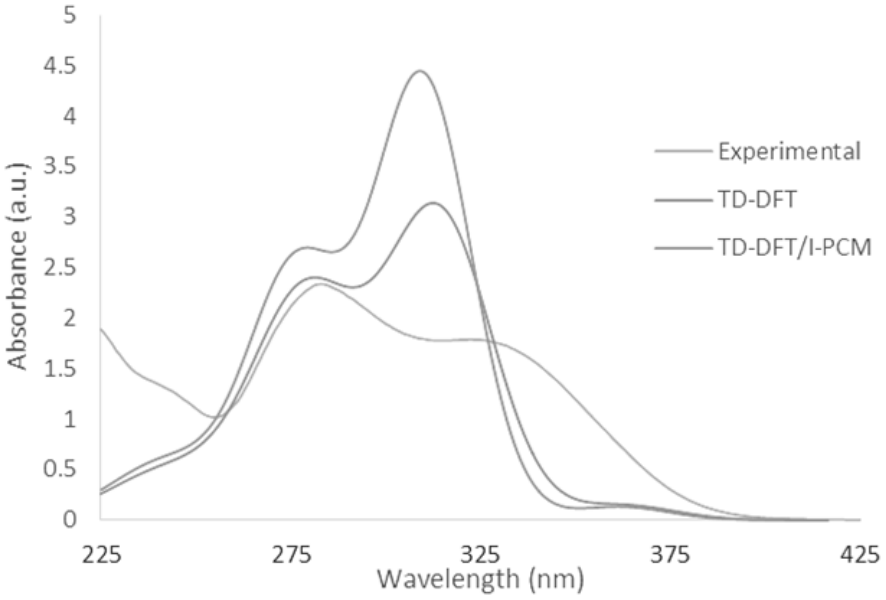

Fig. 3 – The experimental and the simulated UV-Vis spectra of HBC.

Table 3

Experimental and calculated absorption wavelength (nm), excitation energies E(eV) and oscillator strengths (f)

Experimental	TD-DFT			TD-DFT/I-PCM		
λ(nm)	λ(nm)	E(eV)	f	λ(nm)	E(eV)	f
	362(53→55)	3.4237	0.0148	362(53→55)	3.4213	0.0093
330	314(54→55)	3.9511	0.3034	309(54→55)	4.0139	0.3454
284	278(52→55)	4.4519	0.2224	275(52→55)	4.4995	0.1855
	245(54→56)	5.0496	0.0382	245(54→58)	5.0511	0.0333
	238(54→57)	5.2114	0.0024	234(52→57)	5.2965	0.001
	231(53→56)	5.3635	0.0126	232(53→56)	5.3447	0.015

NBO analysis

To have a better understanding of the electronic interactions (charge transfer or conjugative interaction) that occur in the HBC molecule, NBO analysis has been performed at DFT level. Results are presented in Table 4. From the second order perturbation theory analysis results in information on the measure of the stabilization due to the electron transfer from a filled orbital (the donor) to an empty orbital (acceptor). A larger E(2) values means a more intensive interaction between electron donors and electron acceptors, therefore a greater extent of conjugation.[19]

The NBO analysis of the donor-acceptor interactions shows that the most important charge transfer interactions occur in the π-regions and around the O atoms, because of their lone pairs.

The (π) $C_1 - C_2$, (π) $C_3 - C_5$, (π) $C_4 - C_6$ participate as donors and (π^*) $C_3 - C_5$, (π^*) $C_4 - C_6$, (π^*) $C_1 - C_2$ as acceptors within the phenyl group. These conjugative interactions reveal the strong delocalization on the π-conjugation path. The donor-acceptor interactions (π) $C_1 - C_2 \leftrightarrow$ (π^*) $C_7 - C_{13}$ and (π) $C_7 - C_{13} \leftrightarrow$ (π^*) $C_{11} - O_{27}$, having a stabilization energy of 11.11 kcal/mol and 18.63 kcal/mol, respectively, show the presence of an extended conjugation in the HBC molecule. The intramolecular charge transfer, from O_{14} to O_{27}, is supported by the donor-acceptor interaction (LP) $O_{14} \leftrightarrow$ (π^*) $C_4 - C_6$, with a stabilization energy, E(2), of 28.00 kcal/mol. Other important donor-acceptor interactions which contribute to the molecular stabilization are (LP_2) $O_{27} \leftrightarrow$ (σ^*) $C_9 - C_{11}$ and (LP_2) $O_{27} \leftrightarrow$ (σ^*) $C_{11} - C_{13}$.

The Mulliken atomic charges of HBC were calculated at B3LYP/6-311+G(d,p) level of theory. The charge distribution is presented in Fig. 4.

Table 4

Selected NBO analysis of HBC

Donor-acceptor interaction	Occupancy	E(2) (kcal/mol)	E(j) – E(i) (a.u.)	F(i, j) (a.u.)
(π) $C_1 - C_2 \leftrightarrow$ (π^*) $C_3 - C_5$	1.649 ↔ 0.353	18.58	0.28	0.064
(π) $C_1 - C_2 \leftrightarrow$ (π^*) $C_4 - C_6$	1.649 ↔ 0.378	23.15	0.27	0.071
(π) $C_1 - C_2 \leftrightarrow$ (π^*) $C_7 - C_{13}$	1.649 ↔ 0.109	11.11	0.32	0.056
(π) $C_3 - C_5 \leftrightarrow$ (π^*) $C_1 - C_2$	1.662 ↔ 0.382	22.65	0.28	0.072
(π) $C_3 - C_5 \leftrightarrow$ (π^*) $C_4 - C_6$	1.662 ↔ 0.378	17.87	0.27	0.063
(π) $C_4 - C_6 \leftrightarrow$ (π^*) $C_1 - C_2$	1.658 ↔ 0.382	15.77	0.30	0.062
(π) $C_4 - C_6 \leftrightarrow$ (π^*) $C_3 - C_5$	1.658 ↔ 0.353	22.72	0.29	0.073
(π) $C_7 - C_{13} \leftrightarrow$ (π^*) $C_{11} - O_{27}$	1.841 ↔ 0.145	18.63	0.30	0.067
(LP) $O_{14} \leftrightarrow$ (π^*) $C_4 - C_6$	1.873 ↔ 0.378	28.00	0.35	0.095
(LP_1) $O_{27} \leftrightarrow$ (RY^*) C_{11}	1.978 ↔ 0.016	15.55	1.58	0.14
(LP_2) $O_{27} \leftrightarrow$ (σ^*) $C_9 - C_{11}$	1.887 ↔ 0.057	19.13	0.65	0.101
(LP_2) $O_{27} \leftrightarrow$ (σ^*) $C_{11} - C_{13}$	1.887 ↔ 0.070	19.28	0.69	0.104
(π^*) $C_1 - C_2 \leftrightarrow$ (π^*) $C_7 - C_{13}$	0.382 ↔ 0.109	34.53	0.03	0.062
(π^*) $C_4 - C_6 \leftrightarrow$ (π^*) $C_1 - C_2$	0.378 ↔ 0.382	273.06	0.01	0.082
(π^*) $C_{11} - O_{27} \leftrightarrow$ (π^*) $C_7 - C_{13}$	0.145 ↔ 0.109	23.40	0.03	0.068

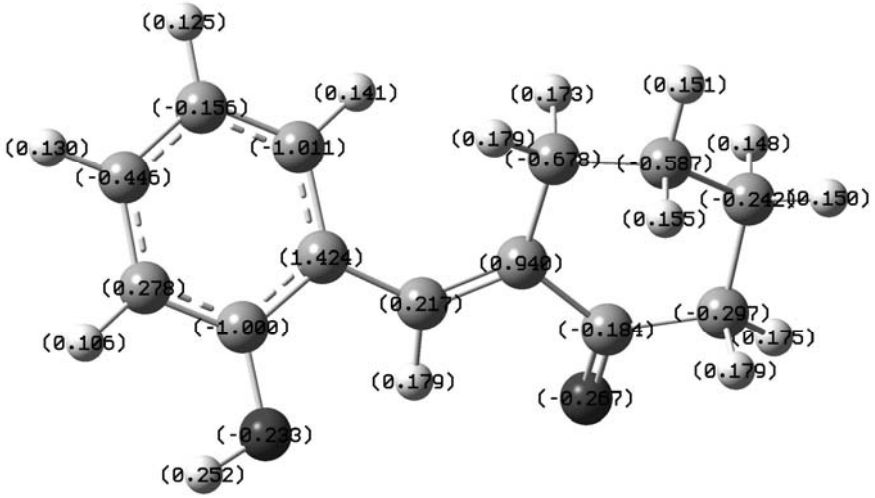

Fig. 4 – The Mulliken atomic charges of HBC at B3LYP/6-311+G(d,p) level of theory.

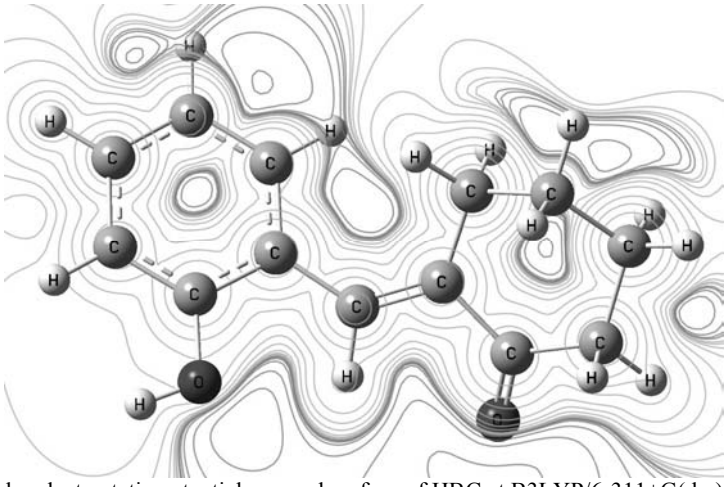

Fig. 5 – Molecular electrostatic potential mapped surface of HBC at B3LYP/6-311+G(d,p) level of theory.

The molecular electrostatic potential (MEP) is a property with a clear physical meaning: it expresses the net electrical effect of the electrons and nuclei of a system in the surrounding space.[20] An important characteristic of the electrostatic potential is that it can be determined experimentally by diffraction methods, as well as computationally.[21] ESP is used to explain and quantify reactivity and structure–activity relationship of molecules and correlates with electronegativity, partial charges and site of chemical reactivity of the molecule.[22] Three important features are usually linked to the negative regions in the electrostatic potential surface: heteroatoms with lone pairs, π regions of unsaturated molecules and bond regions of strained hydrocarbons.[21]

The molecular electrostatic potential mapped surface of HBC at B3LYP/6-311+G(d,p) level of theory is shown in Fig. 5. The regions with negative ESP, corresponding to the areas of high electron density, are represented with red color and the positive valued regions, areas of lowest electron density, with deep blue to indigo color. Green represents regions of zero potential.

From Fig. 5 it is visible that the regions of the most negative electrostatic potential are around the O_{14} atom from the hydroxyl group and the O_{27} atom of the carbonyl group, because of their lone pairs. The electrostatic potential surface presents two more red colored regions, due to the presence of extended conjugation (π regions) and the strained end of cyclohexanone, opposite to the carbonyl group.

HOMO-LUMO energy

The frontier molecular orbitals, HOMO and LUMO, are of great importance because they determine the way the molecule interacts with other species. The HOMO characterizes the electron donor ability, while LUMO the electron acceptor ability. The HOMO-LUMO energy gap is a reactivity descriptor associated with the stability of a compound.[23] The HOMO and LUMO orbitals are presented in Fig. 6.

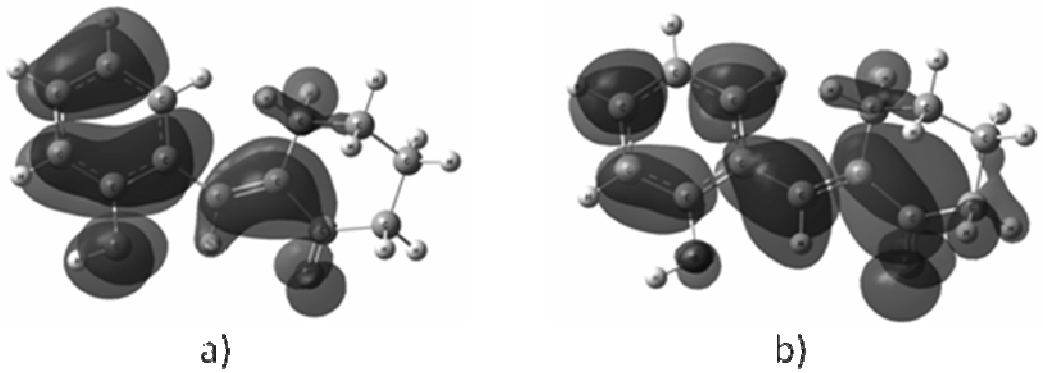

Fig. 6 – The HOMO (a) and LUMO (b) surfaces at B3LYP/6-311+G(d,p) level of theory.

A strong delocalization of both HOMO and LUMO on the π-conjugation path can be observed. The energy values of HOMO and LUMO were calculated at B3LYP/6-311+G(d,p) level of theory: -6.247 eV (HOMO) and -1.923 eV (LUMO). The relative small HOMO-LUMO energy gap, 4.324 eV, is characteristic for a conjugated molecule and explains the possible intramolecular charge transfer from the electron-donor group (hydroxyl) to the electron-acceptor one (the oxygen atom of the carbonyl group).[24]

EXPERIMENTAL

The 2-(2-hydroxy-benzylidene)-cyclohexanone (HBC) was synthesized following a literature protocol.[25] The IR spectrum was recorded on a Jasco 400 spectrometer. The standard KBr technique was used. The UV-Vis absorption spectrum was recorded on an Agilent Technologies Cary 60 UV-Vis spectrophotometer on a $2 \cdot 10^{-4}$M solution of 2-(2-hydroxy-benzylidene)-cyclohexanone in methanol.

Computational details

The HBC structure was geometrically optimized at B3LYP/6-311+G(d,p) level of theory.

The optimized structure was an energy minimum with no imaginary frequencies. The vibrational frequencies were computed and scaled with the appropriate scaling factor 0.9613 to counteract the errors caused by neglecting anharmonicity and electron correlation.[26] The UV-Vis absorption spectra were computed with the time-dependent density functional method TD-DFT/ 6-311+G(d,p). For TD-DFT the PCM (polarizable continuum model) was used to take into account the solvent effects that modify the UV spectra.[27-29] All calculations were performed with the Gaussian 09 program package.[30]

CONCLUSIONS

We have synthesized and characterized 2-(2-hydroxy-benzylidene)-cyclohexanone (HBC). Vibrational and electronic spectral analysis of HBC were performed using FT-IR and UV-Vis spectroscopic techniques. On the basis of the calculated and experimental results, assignment of the fundamental frequencies and absorption wavelengths were examined. The optimized structure of HBC shows a slightly changed chair conformation of the cyclohexanone ring, with the ketone group side a little bit flattened. The theoretical results were compared with the available experimental data for a similar compound. The calculated HOMO and LUMO energies show that charge transfer occurs within the molecule on the O_{14} to O_{27} path. Overall, good quality correlations with the experiments are obtained. From the quantitative point of view, a full agreement is difficult to achieve usually due to errors associated with method and basis set.

REFERENCES

1. B.L. Feringa (Ed.), "Molecular Switches", Wiley-VCH GmbH, Weiheim, Germany, 2011.
2. V. Balzani, M. Venturi and A. Credi, "Molecular Devices and Machines: A journey into the nanoworld", Wiley-VCH GmbH, Weiheim, Germany, 2003.
3. V. Balzani, A. Credi and M. Venturi, "Molecular Devices and Machines; Concepts and Perspectives for the Nanoworld", Wiley-VCH GmbH, Weinheim, Germany, 2008, p. 1-546.
4. J.C. Crano and R.J. Guglielmetti, "Organic Photochromic and Thermochromic Compounds", vol. I "Main Photochromic Families", Plenum Press, New York, USA, 1999.
5. A.M. Diniz, C. Pinheiro, V. Petrov, A.J. Parola and F. Pina, *Chem. Eur. J.*, **2011**, *17*, 6359–6368.
6. H. Horiuchi, H. Shirase, T. Okutsu, R. Matsushima and H. Hiratsuka, *Chem. Lett.*, **2000**, *29*, 96–97.
7. K. Tokumura, N. Taniguchi, T. Kimura and R. Matsushima, *Chem. Lett.*, **2001**, *30*, 126–127.
8. F. Pina, M.J. Melo, C.A.T. Laia, A.J. Parola and J.C. Lima, *Chem. Soc. Rev.*, **2012**, *41*, 869–908.
9. A. Roque, F. Pina, S. Alves, R. Ballardini, M. Maestri and V. Balzani, *J. Mater.Chem.*, **1999**, *9*, 2265–2269.
10. Z. Jia, J.W. Quail and J.R. Dimmock, *Acta Cryst.*, **1990**, C46, 2467–2468.
11. J.C. Tai and N.A. Allinge, *J. Am. Chem. Soc.*, **1966**, *88*, 2179.
12. P.D. Vaz and P.J.A. Ribeiro-Claro, *J. Raman Spectrosc.* 2003; **34**: 863.
13. B. Smith, Infrared Spectral Interpretation, A Systematic Approach, CRC Press, Washington, DC, 1999.
14. D. Lin-Vein, N.B. Colthup, W.G. Fateley and G.J. Grasselli, "The Handbook of Infrared and Raman Characteristic Frequencies of Organic Molecules", Academic Press, New York, 1991.
15. H. Fuhrer, V.B. Kartha, P.J. Krueger, H.H. Mantsch and R.N. Jones, *Chem. Rev.*, **1972**, *72*, 439.
16. C. James, A. Amal Raj, R. Reghunathan, V.S. Jayakumar and I. Hubert Joe, *J. Raman Spectrosc.*, **2006**, *37*, 1381.
17. D. Sajan, I. Hubert Joe, V.S. Jayakumar and J. Zaleski, *J. Mol. Struct.*, **2006**, *785*, 43.
18. S. Gunasekaran and S. Ponnusamy, *Indian J. Pure Ap. Phy.*, **2005**, *43*, 838–843.
19. E.D. Glendening, J.K. Badenhoop, A.E. Reed, J.E. Carpenter, J.A. Bohmann, C.M. Morales and F. Weinhold, NBO 5. 0, Theoretical Chemistry Institute, University of Wisconsin, Madison, 2001.
20. P. Politzer, P.R. Laurence and K. Jayasuriya, *Environ. Health Persp.*, **1985**, *61*, 191–202.
21. J.S. Murraz, J.M. Seminario, M.C. Concha and P. Politzer, *Int. J. Quant. Chem.*, **1992**, *44***,** 113–122.
22. D. Sajan,d, K. Udaya Lakshmi, Y. Erdogdu and I. Hubert Joe, *Spectrochim. Acta A*, **2011**, *78*, 113–121.
23. F. De Proft and P. Geerlings, *Chem. Rev.*, **2001**, *101*, 1451–1464.

24. C.H. Choi and M. Kertesz, *J. Phys. Chem. A*, **1997**, *101*, 3823.
25. J.R. Dimmock, P.Kumar, A.J. Nazarali, N.L. Motaganahalli, T.P. Kowalchuk, M.A. Beazely, J.W. Quail, E.O. Oloo, T.M. Allen, J. Szydlowski, E. DeClercq and J. Balzarini, *Eur. J. Med. Chem.*, **2000**, *35*, 967–977.
26. A.P. Scott and L. Radom, *J. Phys. Chem.*, **1996**, *100*, 16503.
27. M. Cossi and V. Barone, *J. Chem. Phys.*, **2001**, *115*, 4708.
28. C. Amovilli, V. Barone, R. Cammi, E. Cancès, M. Cossi, B. Mennucci, C.S. Pomelli and J. Tomasi, *Adv. Quantum Chem.*, **1998**, *32*, 227.
29. J. Tomasi, B. Mennucci and R. Cammi, *Chem. Rev.*, **2005**, *105*, 2999.
30. Gaussian 09, Revision B.01, M. J. Frisch, G. W. Trucks, H. B. Schlegel, G. E. Scuseria, M. A. Robb, J. R. Cheeseman, G. Scalmani, V. Barone, B. Mennucci, G. A. Petersson, H. Nakatsuji, M. Caricato, X. Li, H. P. Hratchian, A. F. Izmaylov, J. Bloino, G. Zheng, J. L. Sonnenberg, M. Hada, M. Ehara, K. Toyota, R. Fukuda, J. Hasegawa, M. Ishida, T. Nakajima, Y. Honda, O. Kitao, H. Nakai, T. Vreven, J. A. Montgomery, Jr., J. E. Peralta, F. Ogliaro, M. Bearpark, J. J. Heyd, E. Brothers, K. N. Kudin, V. N. Staroverov, T. Keith, R. Kobayashi, J. Normand, K. Raghavachari, A. Rendell, J. C. Burant, S. S. Iyengar, J. Tomasi, M. Cossi, N. Rega, J. M. Millam, M. Klene, J. E. Knox, J. B. Cross, V. Bakken, C. Adamo, J. Jaramillo, R. Gomperts, R. E. Stratmann, O. Yazyev, A. J. Austin, R. Cammi, C. Pomelli, J. W. Ochterski, R. L. Martin, K. Morokuma, V. G. Zakrzewski, G. A. Voth, P. Salvador, J. J. Dannenberg, S. Dapprich, A. D. Daniels, O. Farkas, J. B. Foresman, J. V. Ortiz, J. Cioslowski, and D. J. Fox, Gaussian, Inc., Wallingford CT, **2010**.